

SAPOTI - THE NEW CRYOGENIC NANOPROBE FOR THE CARNAÚBA BEAMLINE AT SIRIUS/LNLS

R.R. Geraldes[†], F.R. Lena, G.G. Basilio, D.N.A. Cintra, V.B. Falchetto, D. Galante,
R.C. Gomes, A.Y. Horita, L.M. Kofukuda, M.B. Machado, Y.A. Marino, E.O. Pereira, C.A. Pérez,
P.P.R. Proença, M.H. Siqueira da Silva, A.P.S. Sotero, V.C. Teixeira, H.C.N. Tolentino
Brazilian Synchrotron Light Laboratory (LNLS), Campinas, São Paulo, Brazil

Abstract

SAPOTI will be the second nanoprobe to be installed at the CARNAÚBA (Coherent X-Ray Nanoprobe Beamline) beamline at the 4th-generation light source Sirius at the Brazilian Synchrotron Light Laboratory (LNLS). Working in the energy range from 2.05 to 15 keV, it has been designed for simultaneous multi-analytical X-ray techniques, including absorption, diffraction, spectroscopy, fluorescence and luminescence, and imaging in 2D and 3D. Highly-stable fully-coherent beam with monochromatic flux up to 10^{11} ph/s/100mA/0.01%BW and size between 35 and 140 nm is expected with an achromatic KB (Kirkpatrick-Baez) focusing optics, whereas a new in-vacuum high-dynamic cryogenic sample stage has been developed aiming at single-nanometer-resolution images via high-performance 2D mapping and tomography. This work reviews and updates the entire high-performance mechatronic design and architecture of the station, as well as the integration results of some of its modules, including automation, thermal management, dynamic performance, and positioning and scanning capabilities. Commissioning at the beamline is expected in early 2024.

INTRODUCTION

Synchrotron scanning X-ray microscopy has been established as a mature technique and a key characterization tool for scientific, technological, and engineering fields, with several beamline X-ray microscopes with beams of nanometric sizes (a.k.a. nanoprobes) being developed during this decade [1-11]. In particular, complementing techniques such as ultra-high-resolution fluorescence, the use of ptychography as a coherent X-ray diffractive imaging technique enables single-digit nanometer level spatial resolution, ultimately limited only by the beam and the sample stability during the exposure time [5, 7, 8, 11-13].

SAPOTI will be the second nanoprobe to be installed at the CARNAÚBA (Coherent X-Ray Nanoprobe Beamline) beamline at the 4th-generation light source Sirius at the Brazilian Synchrotron Light Laboratory (LNLS) [14, 15]. It has been designed for simultaneous multi-modal state-of-the-art X-ray techniques, including absorption, diffraction, spectroscopy, fluorescence and luminescence, and imaging in 2D and 3D. At 142 m from the undulator source and with achromatic optics, full benefit can be taken from

the brilliance of the new-generation storage ring to reach diffraction-limited beam sizes, from 140 to 35 nm in the energy range from 2.05 to 15 keV, while optimizing the photon flux up to 10^{11} ph/s/100 mA/0.01%BW at the sample.

As comprehensively described in [15] and depicted in Fig. 1, SAPOTI will be an all-in-vacuum station, with a Kirkpatrick-Baez (KB) set of mirrors and the sample stage sharing the same ultra-high vacuum chamber. This architectural decision was made for stability, metrology and alignment purposes, and for optimization of transmission in the low-energy end. Three photodiodes (PD) for flux and absorption measurements, as well as two silicon drift detectors (SDDs) for fluorescence, are also placed inside the chamber, whereas the area detector (PiMEGA) and a complementary optical arrangement, alternatively used for an optical or a luminescence (X-ray Excited Optical Luminescence – XEOL) microscope, are placed outside vacuum, accessing the sample signals via a large beryllium window and a small glass viewport, respectively. Above the main chamber, a loading chamber comprises a load-lock system for cryogenic sample transfer, a cryogenic parking station (carousel) for sample storage, and a cryogenic pick-and-place gripper mechanism for sample loading. Cryogenic cooling at both the sample stage in main chamber and the parking station in the loading chambers is achieved by means of efficient thermal management using two pulse tube (PT) coolers.

Since the beginning of the project, the main aspect driving its mechatronic architecture has been the extreme sensitivity of the focusing optics and the sample to mechanical stability, once ultimate mapping resolution is one of the key design targets in the station. Firstly, a granite bench following the concepts developed for Sirius systems provides a stand with high mechanical and thermal stability, while allowing for basic positioning of station with respect to the beam in all degrees of freedom (DoFs) [16, 17]. Next, both the KB module and the sample stage are quasi-directly fixed to the granite bench, i.e., stiffly mounted via the bottom flange of the main chamber. Although unusual for beamline in-vacuum systems, and significantly more challenging in terms of manufacturing, assembly and baking, this solution offers unique possibilities regarding dynamics, i.e., suspension frequencies and vibration amplitudes.

[†] renan.geraldes@lnls.br

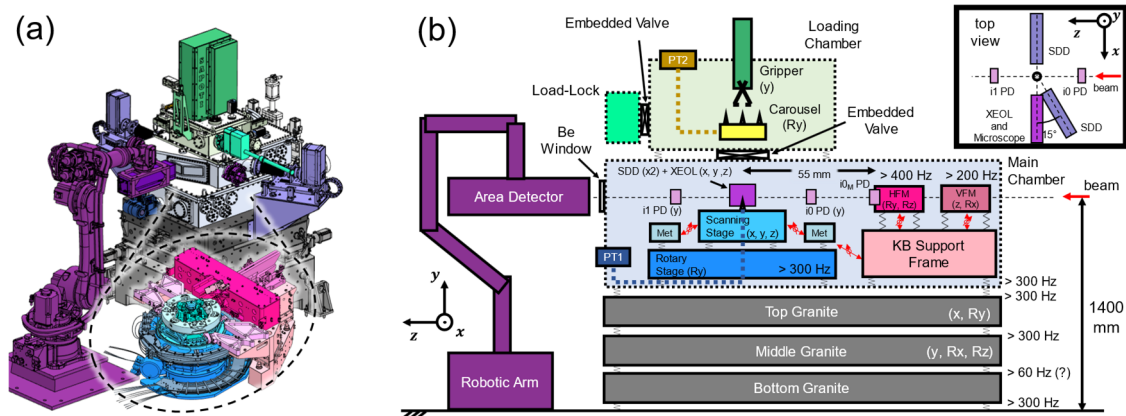


Figure 1: (a) Overview of the SAPOTI station, highlighting a few subsystems: granite bench, chambers, gripper and load-lock, detectors, sample stage and KB module. (b) Schematic overview of the main elements in the station, in color code. Distances, suspension frequencies, motion degrees of freedom and metrology links (red), are indicated for reference.

Indeed, this way these critical modules can benefit from the stiffness and inertia properties of the bench while preventing the use of long feedthrough structures via bellows. The KB design follows the exactly-constrained (isostatic) solution that has been recently developed for Sirius KB mirrors, in which flexural struts are combined with piezo actuators in optimized configurations [18]. The sample stage, in turn, follows a high-dynamic mechatronic concept, according to an isolated mechatronic architecture with high-bandwidth closed-loop control [19]. Using voice-coils actuators, laser interferometer feedback, a reaction mass working as a dynamic filter, and a set of folded-leafsprings acting as a parallel-kinematic arrangement, it allows for a relatively large stroke of 3 mm XYZ, while keeping positioning errors around 1 nm RMS (up to 10 kHz) and reaching scanning speeds up to hundreds of micrometers per second. Below the high-performance scanning stage, a rotary stage allows for tomography over 220°.

The following section is dedicated to the latest updates in design and experimental data (refer also to [15, 19]). Then, conclusions are summarized in the last section.

DESIGN AND INTEGRATION STATUS

Most of the design work for SAPOTI has been concluded. Thus, its modules are either in final manufacturing stage or already under assembly and integration in a clean-room in the Metrology Building at the LNLS. The following sub-sections highlight the main updates for the system.

Pulse Tube Coolers

Given the low power extraction requirements for sample conditioning, together with their cost and/or operation advantages as compared to either open-circuit cryostats and closed-loop liquid nitrogen cryocoolers, helium gas closed-circuit pulse tube coolers are used as compact stand-alone systems both with the sample stage in the main chamber and the carousel in the loading chamber (see Fig. 1).

A potential issue, however, might be related to mechanical disturbances introduced by the systems compressors. In that sense, the first step was the selection of the low-

vibration model LPT9310 by Thales Cryogenics. Relying on a pair of voice-coil actuators and flexural bearings, it provides an anti-vibration operation mode (AVR), in which a feedback loop with an accelerometer can be used to balance the magnitude and phase of the actuators and thus minimize vibrations [20]. A second action point was including in the design a decoupling solution at about 15 Hz for the mounting structure of the compressor, such that forces at higher frequencies can be passively filtered.

Figure 2 shows the mechanical assembly of one of the coolers and a vibration measurement plot. The AVR lowers the acceleration peaks of the first modes, which not only leads to lower amplitudes but also can be more efficiently filtered by the decoupling parallel flexures. One important remark is that the AVR is only effective once the heat pumping capacity is not saturated, i.e., the temperature setpoint of the cold finger can be achieved by the controller.

For the heat extraction needs for SAPOTI around 2 to 2.5 W, and temperatures around 20 to 35 °C in the reservoir and compressor (maintained via water cooling), the measurements resulted in 60 to 70 K as achievable targets. User interfaces and software layers for EPICS have been developed in house, and the units are ready for final integration.

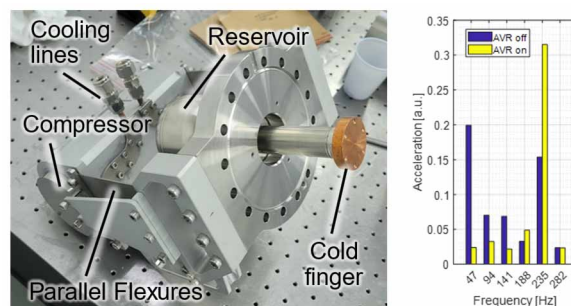


Figure 2: Pulse tube cooler LPT9310 mechanical assembly on a bench. Details drawn to its cold finger, reservoir and compressor, and the proposed mounting structure with decoupling flexures and cooling lines. The plot shows normalized acceleration levels at the multiple harmonics of the system, both with the anti-vibration system on and off.

KB Module

A comprehensive description of the KB module global design and its specifications (with stability requirements as low as 4 nrad) can be found in [15]. Now, having finished its detailed design, the VFM (vertical-focusing mirror) is expected to achieve a motion range of 20 μ rad and resolution of 20 nrad in pitch using a PIRest actuator, and a range of 250 μ m and resolution of 10 nm in using a piezomike actuator. Modal analyses predict that its first suspension mode will be around 230 Hz, whereas first pitch mode above 650 Hz. As for the HFM (horizontal-focusing mirror), it is expected to achieve a motion range of 50 μ rad and resolution of 50 nrad in pitch using a PIRest actuator, and 1.2 mrad of range and 80 nrad of resolution in using a piezomike actuator. Modal analyses predict that its first suspension mode will be around 400 Hz, whereas the first pitch mode above 600 Hz. Figure 3 depicts the structural simulation for these alignment DoFs.

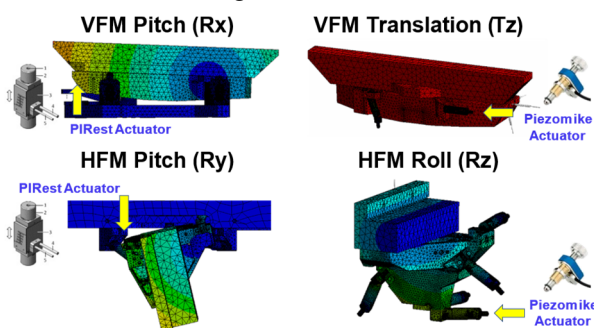


Figure 3: Structural simulations illustrating the fine-alignment degrees of freedom of the KB vertical- and horizontal-focusing mirror (VFM and HFM) mechanisms, designed for high suspension frequencies.

Regarding the main support frame (see Fig. 1), according to final simulations (including the masses of the VFM and HFM) the first suspension frequencies are expected around 300 to 400 Hz, which is sufficiently high for most environmental and operational disturbances, while limited by mass and mounting interface stiffnesses. The module parts are under manufacture and expected to be integrated and experimentally validated in the coming months.

Sample Stage

The design and preliminary results of the high-dynamic cryogenic sample stage developed for SAPOTI have been discussed in detail in [15, 19]. Regarding the reported limitations in thermal management, previously limiting the sample temperatures above 135 K, design upgrades have been proposed and partially validated in parallel setups, suggesting that 95 to 100 K shall be now practically achievable – which is critical for sample preservation against crystalline ice. More information on this, together with validation data, will be provided in a future publication. Here, more attention is dedicated to the updates in motion.

Figure 4 shows the open loop Bode plot of the three XYZ scanning DoFs according to the latest SISO (single-input-single-output) control proposal. As in [19], the characteris-

tics of the system at different working points can be distinguished. And, now, by extending the working range from a sphere of 1.5 mm to 2 mm of radius, larger plant variations can be observed. They result from non-linearities in the system, such as changes in the stiffness of the folded-leaf-springs, in the inertia of short-stroke module and in the gains of the voice-coil actuators (see [19]). Hence, in addition to more or less impactful dynamics variations that must be considered in the controller for each DoF, this translates to bandwidth variations by as much as 100 Hz, between 100 and 300 Hz, for the different DoFs. These aspects can be taken into account by more sophisticated control strategies, but this has not proven necessary thus far, with sufficiently performing and robust operation.

Another instructive fact learned recently is related to the first bandwidth-limiting resonances in x and z , indicated by the arrows in Fig. 4. In [19], they had been misleadingly credited to limited stiffness in the bend of the folded leaf-springs, as compared to the original model. After some experimental evaluation, however, they proved to be related to previously unmodelled dynamics. In x , the root cause has been identified as internal modes in the folded leaf-springs, whereas in z it seems that internal dynamics in the flexural cooling core is to blame, which reinforces the importance of and the sensitivity to every design detail in advanced mechatronic systems. These remaining dynamics would require deeper design rework to be solved, which does not seem needed for the moment. Yet, this learning process has increased design awareness for possible future upgrades and future projects.

While its software migration to NI's cRIO final platform is ongoing, the sample stage continues to be operated with a Speedgoat's xPC prototyping platform at 20 kHz (see [19]). In the meantime, some work has been done on high-performance 2D scanning using feedforward control. Figure 5 summarizes a study contemplating 4 raster fly-scan scenarios, all of them taking 50 % overlap for ptychography and 1 kHz detection rate, namely: (i) 20 \times 20 μ m² out-of-focus (500 μ m beam) scan for coarse mapping (maximum speed); (ii) standard 7.5 \times 7.5 μ m² high-resolution low-energy (120 nm beam) scan; (iii) short-range 1 \times 1 μ m² low-energy (120 nm beam) scan; and (iv) standard 1.5 \times 1.5 μ m² high-resolution high-energy (30 nm beam) scan. As an example, the main plot shows the XY reference and the metrology signals for (iv) (in a similar representation to that of [9]). The colors show the sections of each acquisition interval of 1 ms, which are used to the RMS errors statistics of the histogram in the inset. The full 2D map is extracted in only 6.4 s, with a mean RMS error of about 1.25 nm. Hence a full high-resolution tomogram might take less than one hour to be acquired, allowing for high throughput at beamline.

The embedded table outlines the parameters of all trajectories (with the RMS values taken over the full dataset). All scans can be performed within 10 s (with (iii) taking only 0.2 s) with average RMS errors always below 4 nm. The stage is still mounted to an optical table in the metrology room, so that final performances will be reached once the stage is mounted in vacuum and coupled to the bench.

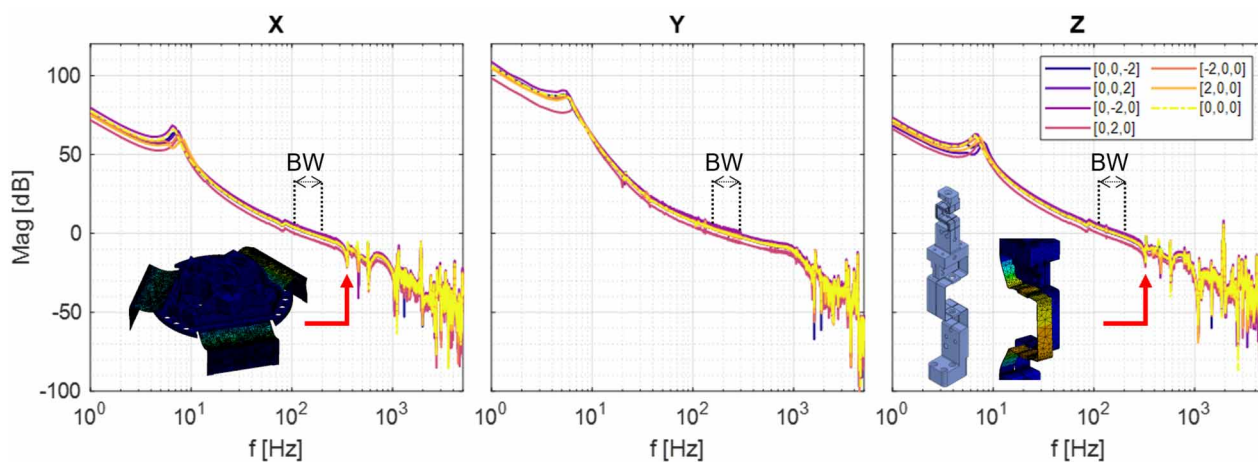
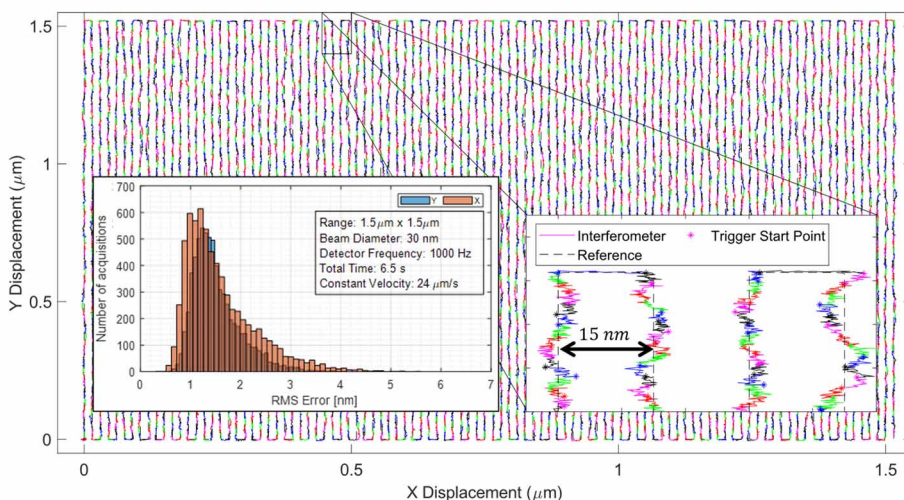


Figure 4: Open loop Bode plot for the x , y and z degrees of freedom of the SAPOTI sample stage for plants measured at an extended working range of ± 2 mm in all directions (coordinates shown as $[x,y,z]$). Modal analysis simulations and experimental tests indicate unpredicted internal modes affecting achievable control bandwidth in x and z .



Trajectory	i	ii	iii	iv
Range [$\mu\text{m} \times \mu\text{m}$]	20x20	7.5x7.5	1x1	1.5x1.5
Velocity [$\mu\text{m/s}$]	260	94	94	23.5
Total Time [s]	7.7	10	0.2	6.4
X_{RMS} [nm]	3.9	2.5	3.1	1.7
Y_{RMS} [nm]	3.1	2.4	2.7	1.6
X_{p2p} [nm]	32.5	23.5	19.6	15.3
Y_{p2p} [nm]	32.1	20.9	18.2	13.5

Figure 5: Trajectory performance analyses for SAPOTI's sample stage, including coarse mapping and low- and high-energy fly-scan scenarios (see text). The table shows range, velocity and scan time, as well as RMS and peak-to-peak (p2p) position errors. The plot depicts the high-energy high-performance raster scan (iv) with a histogram for statistics.

CONCLUSIONS

This work provides an updated overview and the status of the forthcoming SAPOTI cryogenic nanoprobe at the CARNAÚBA beamline at Sirius/LNLS. As the design work ends, and its modules are integrated, the multi-modal, high-throughput and high-resolution imaging requirements are gradually validated, thanks to a systematic design approach, based on high-performance mechatronics and systems engineering concepts and tools. The main next steps include: the conclusion of the software in cRIO; the definitive validation of the new cooling core with the sample stage; the assembly and validation of the KB module, and its integration with the sample stage in the main chamber; and the assembly, validation and integration of the carousel and gripper modules in the loading chamber. First commissioning experiments are expected in June 2024.

ACKNOWLEDGEMENTS

The authors would like to gratefully acknowledge the funding by the Brazilian Ministry of Science, Technology and Innovation, and the contributions of the LNLS and the MI-Partners teams to the instrument. This work is dedicated to the memory of the late team member and dear friend João Leandro de Brito Neto.

REFERENCES

- [1] L. Mino *et al.*, "Materials Characterization by Synchrotron X-ray Microprobes and Nanoprobes", *Rev. Mod. Phys.*, vol. 90, pp. 25–30, 2018. doi:10.1103/revmodphys.90.025007
- [2] R. Winarski *et al.*, "A Hard X-ray Nanoprobe Beamline for Nanoscale Microscopy", *J. Synchrotron Radiat.*, vol. 19, pp. 1056–1060, 2012. doi:10.1154/1.2951844

- [3] S. Chen *et al.*, “The Bionanoprobe: Hard X-ray Fluorescence Nanoprobe with Cryogenic Capabilities”, *J. Synchrotron Radiat.*, vol. 21, pp. 66–75, 2014. doi:10.1107/s1600577513029676
- [4] G. Martínez-Criado *et al.*, “ID16B: a Hard X-ray Nanoprobe Beamline at the ESRF for Nano-Analysis”, *J. Synchrotron Radiat.*, vol. 23, pp. 344–352, 2016. doi:10.1107/s1600577515019839
- [5] E. Nazaretski *et al.*, “Design and Performance of an X-ray Scanning Microscope at the Hard X-ray Nanoprobe Beamline of NSLS-II”, *J. Synchrotron Radiat.*, vol. 24, pp. 1113–1119, 2017. doi:10.1107/s1600577517011183
- [6] R. S. Celestre *et al.*, “Nanosurveyor 2: A Compact Instrument for Nano-Tomography at the Advanced Light Source”, *J. Phys. Conf. Ser.*, vol. 849, p. 012047, 2017. doi:10.1088/1742-6596/849/1/012047
- [7] F. Villar *et al.*, “Nanopositioning for the ESRF ID16A Nano-Imaging Beamline”, *Synchrotron Radiat. News*, vol. 31, pp. 9–14, 2018. doi:10.1080/08940886.2018.1506234
- [8] M. Holler *et al.*, “OMNY – A toMographic Nano crYo stage”, *Rev. Sci. Instrum.*, vol. 89, p. 043706, 2018. doi:10.1063/1.5020247
- [9] J. Deng *et al.*, “The Velociprobe: an Ultrafast Hard X-ray Nanoprobe for High-Resolution Ptychographic Imaging”, *Rev. Sci. Instrum.*, vol. 90, p. 083701, 2019. doi:10.1063/1.5103173
- [10] M. Osterhoff *et al.*, “Focus Characterization of the NanoMAX Kirkpatrick-Baez Mirror System”, *J. Synchrotron Radiat.*, vol. 26, pp. 1173–1180, 2019. doi:10.1107/s1600577519003886
- [11] A. Schropp *et al.*, “PtyNAMi: Ptychographic Nano-Analytical Microscope”, *J. Appl. Cryst.*, vol. 53, pp. 957–971, 2020. doi:10.1063/1.5103173
- [12] H. N. Chapman and K. A. Nugent, “Coherent Lensless X-ray Imaging”, *Nat. Photonics*, vol. 4, p. 833, 2010. doi:10.1038/nphoton.2010.240
- [13] A. M. Maiden *et al.*, “An Annealing Algorithm to Correct Positioning Errors in Ptychography”, *Ultramicroscopy*, vol. 120, pp. 64–72, 2012. doi:10.1016/j.ultramicro.2012.06.001
- [14] H. C. N. Tolentino *et al.*, “The CARNAÚBA X-ray nanospectroscopy beamline at the Sirius-LNLS synchrotron light source: Developments, commissioning, and first science at the TARUMÃ station”, *J. Electron. Spectrosc. Relat. Phenom.*, vol. 226, p. 147340, 2023. doi:10.1016/j.eispec.2023.147340
- [15] R. R. Galdes *et al.*, “The High-Dynamic Cryogenic Sample Stage for the SAPOTI Nanoprobe at the CARNAUBA Beamline at Sirius/LNLS”, *AIP Conf. Proc.*, vol. 2990, p. 040017, 2023. doi:10.1063/5.0168438
- [16] R. R. Galdes *et al.*, “Granite Benches for Sirius X-ray Optical Systems”, in *Proc. of MEDSI'18*, Paris, France, Jun. 2018, pp. 361–364. doi:10.18429/JACoW-MEDSI2018-THPH12
- [17] R. R. Galdes *et al.*, “Design and Commissioning of the TARUMÃ Station at the CARNAÚBA Beamline at Sirius/LNLS”, in *Proc. MEDSI'20*, Chicago, USA, July 2021, pp. 292–295. doi:10.18429/JACoW-MEDSI2020-WEPB13
- [18] G. B. Z. L. Moreno *et al.*, “Exactly-constrained KB Mirrors for Sirius/LNLS Beamlines: Design and Commissioning of the TARUMÃ Station Nanofocusing Optics at CARNAÚBA Beamline”, in *Proc. of MEDSI'20*, Chicago, USA, July 2021, pp. 111–114. doi:10.18429/JACoW-MEDSI2020-TU0B01
- [19] R. R. Galdes *et al.*, “The Sample Positioning Stage for the SAPOTI Nanoprobe at the CARNAÚBA Beamline at Sirius/LNLS”, in *Proc. of 37th ASPE Annual Meeting*, Bellevue, USA, Oct. 2022, pp. 91–97.
- [20] D. L. Johnson *et al.*, “Characterization Testing of the Thales LPT9310 Pulse Tube Cooler”, *Cryocoolers*, vol. 18, pp. 125–133, 2014.